Chapter 5

Characterization of Multiblock (Segmented) Copolyurethane-Imides and Nanocomposites Based Thereof Using AFM, Nanotribology, and Nanoindentation Methods

Tatiana Evgenievna Sukhanova,
Tatyana A. Kuznetsova, Vasilina A. Lapitskaya,
Tatiana I. Zubar, Sergei A. Chizhik,
Milana E. Vylegzhanina, Aleksandr A. Kutin,
Andrey L. Didenko and Valentin M. Svetlichnyi

Additional information is available at the end of the chapter

http://dx.doi.org/10.5772/intechopen.78625

Abstract

This chapter reviews our results on the morphology, tribological, and local mechanical property investigations of new copoly(urethane-imide)s (coPUIs) and nanocomposites based thereof using atomic force microscopy (AFM) and nanoindentation (NI) methods. AFM in the contact mode of lateral forces revealed the presence of different contrast phases on the surface of synthesized films which depends on the chemical structure of monomers used. Single-walled carbon nanotubes (SWCNTs), carbon nanofibers, graphene, tungsten disulfide and tungsten diselenide were introduced into coPUI matrices. Dependencies of microhardness and modulus of elasticity on the depth of indentation have been obtained. It was found that for each synthesized coPUI, there is only one type of carbon nanomaterials that exerts the greatest influence on their characteristics. The improvement of mechanical properties is found to mainly depend on the nature of the polymer matrix and filler. Our results showed that effective methods for improving of tribological characteristics can be either modification by SWCNTs (up to 1 wt.%) or heating at 30°C. Synthesized coPUI films and nanocomposites are very promising materials and can be used as thermoplastic elastomers for tribological applications, and their physical-mechanical properties can be controlled both by temperature and by mechanical action.

Keywords: atomic force microscopy, nanoindentation, nanotribology, copoly(urethane-imide)s, polymer nanocomposites, morphology, local mechanical properties

1. Introduction

For the creation of new-generation polymer materials based on multicomponent systems, it is necessary to study the morphology, mechanical behavior, and various properties of these systems in the submicron and nanoscale range. It is known that surface layers of polymer objects exhibit significant differences in properties as compared with bulk material and play a decisive role in various applications especially if they are used as films and coatings [1].

In recent years, various probe methods have been successfully used for these purposes, among which the most popular are atomic force microscopy (AFM) and nanoindentation (NI) [2, 3]. Atomic force microscopy is an indispensable technique to study the various surface phenomena [4–6]. AFM allows not only to evaluate the roughness of the surface but also recognize the different localized phases and reveal the distribution of friction forces over the surface and evaluate the tribological characteristics of polymer materials in the micro- and nanoscale [6–9].

The aim of this work was to study the morphological, local mechanical, and tribological characteristics of a series of novel multiblock (segmented) copolymers, containing rigid imide blocks and flexible blocks of polyurethanes—copoly(urethane-imide)s (coPUI)s and their nanocomposites—containing carbon nanofillers of different morphologies: single-walled carbon nanotubes (SWCNTs), vapor-grown carbon nanofibers (VGCF), and graphene as well as nanoparticles of transition metal chalcogenides—tungsten disulfide (WS_2) and tungsten diselenide (WSe_2). The synthesized materials were characterized down to the nanoscale level using AFM in contact and tapping modes, including the friction coefficient measurement [10] at the temperature range from 20 up to 120°C and multi-pass friction force determination till 400 scanning fields, and NI method [11] for the local mechanical property evaluation as the dependence of the characteristics on the depth of an indenter penetration.

Multiblock (segmented) copolymers are the block copolymers containing a rigid block of monomer A and a flexible-chain polymer block (B)k ([A–(B)k]n). A characteristic feature of such copolymers is the microphase separation of blocks A and (B)k, since blocks A and (B)k are thermodynamically incompatible [12]. As a result, nano- and micro-regions are formed in the volume of the copolymer, in which segments (blocks) of the same chemical structure are concentrated. Thanks to the microphase separation of the rigid blocks (A) and flexible blocks of aliphatic ethers ((B)k), these copolymers acquire the properties of elastomers: their glass transition temperature (T_g) is in the negative temperature range on the Celsius scale, and the temperature dependencies of the elastic modulus at higher T_g are distinguished by a wide range of rubberlike elasticities, while the relative tensile elongation at room temperature is hundreds of percent [13].

Changing the chemical structure and the ratio of rigid and flexible blocks in coPUIs, one can change the structure, morphology, and mechanical and thermal properties of these

http://dx.doi.org/10.5772/intechopen.78625

polymers [14–17]. Modification of multiblock coPUI with the introduction of carbon and chalcogenide nanosized additives aims to expand their temperature range without losing its elasticity. Finally, the new generation of thermoplastic elastomers for working in the extremal conditions based on multiblock coPUIs intended to be prepared which exhibit unique rubberlike elasticity in a wide range of temperatures and a higher heat resistance than thermoplastic polyurethanes [6, 9, 18–20]. Such materials are very promising for application in airspace technique, shipbuilding and car industry, microelectronics, and membrane technology [21, 22].

2. Experimental details

2.1. Materials

Chemical approaches to the synthesis of multiblock (segmented) copolyester-imides and copolyurethane-imides (coPUIs) are proposed in general form in previous works [23–25]. In these studies, macromonomers with terminal anhydride groups are used which are formed by terminating with tetracarboxylic acid dianhydrides of polyesters having terminal hydroxyl groups (in the case of copolyester-imides) or terminal isocyanate groups (in the case of copolyurethane-imides), respectively. Further, the expansion of the macromonomer chains is carried out using aromatic diamines which interact with their terminal anhydride groups. The polyacylation of diamines with macromonomer dianhydrides is carried out according to schemes known in the chemistry of polyimides.

For the synthesis of new family of multiblock coPUIs, the 1,3-bis-(3′,4-dicarboxy-phenoxy)benzene dianhydride (R) (T_m = 163–165°C, LLC TekhChemProm, Yaroslavl) and diamine1,4′-bis-(4′-aminophenoxy)diphenyl sulfone (diamine SOD) (T_m = 194–196°C, VWR International) with various ester fragments, as well as an aliphatic copolyester-poly(propylene glycol) (PPG) or poly(1,6-hexanediol/neopentyl glycol-alt-adipic acid) (Alt) (900) (T_m = 33°C, M_n = 900, Aldrich), secondarily terminated with 2,4-tolylene diisocyanate (TDI 2300) (T_m = 19.5–21.5°C, M_n = 2300, Aldrich), were used. The chemical structures of the coPUIs are presented in **Schemes 1** and **2**.

Depending on the chemical structure of flexible aliphatic and rigid aromatic blocks, the synthesis of copolymers was carried out according to different schemes.

Synthesis of multiblock (segmented) coPUI (R-AltTDI-R)SOD (**Scheme 1**) includes four stages:

1. The stage of formation of a macromonomer with terminal toluene isocyanate groups (AltTDI).
2. The stage of formation of a macromonomer with terminal anhydride groups (R-AltTDI-R).
3. The step of polyacylation of diamine (expansion of the macromonomer chain) to form a prepolymer-copolyamide acid (R-AltTDI-R)SOD.
4. The stage of thermal imidization of the prepolymer (copolyamide acid) to form copolyurethane-imide (R-AltTDI-R)SOD.

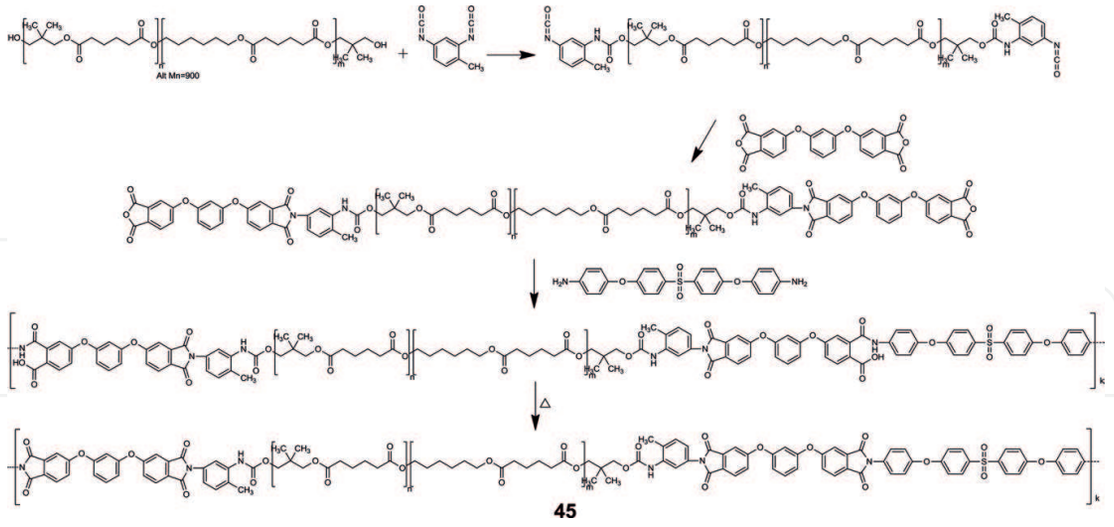

Scheme 1. Schematic representation synthesis of coPUI (R-AltTDI-R)SOD.

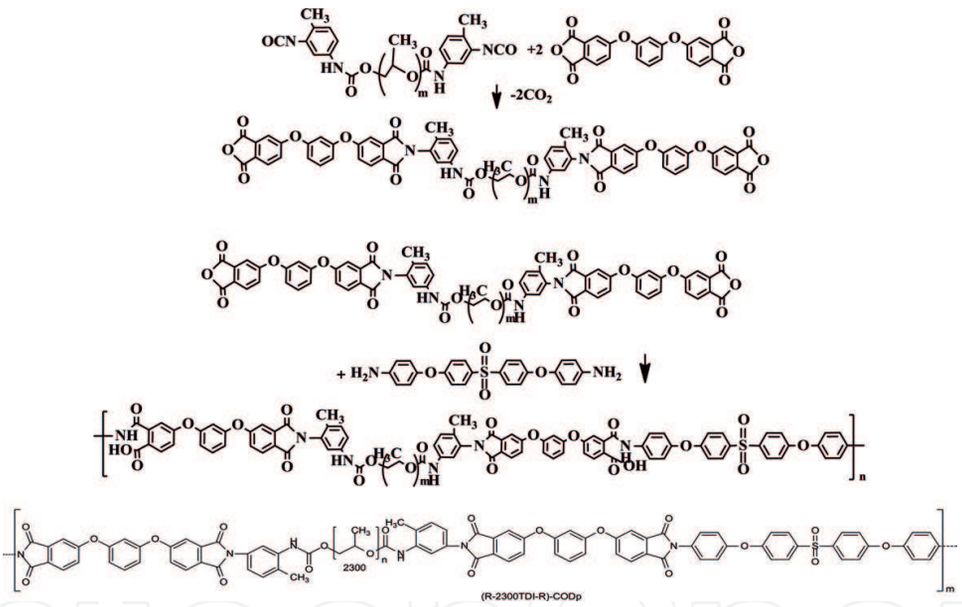

Scheme 2. Schematic representation synthesis of coPUI (R-2300TDI-R)SOD.

Synthesis of multiblock (segmented) coPUI (R-2300TDI-R)SOD includes three stages (**Scheme 2**) as described previously in our papers [6, 19, 23]:

1. The step of forming a macromonomer with terminal anhydride groups (R-2300TDI-R).
2. The step of diamine polyacylation (expansion of the macromonomer chain) to form a prepolymer-copolyamide acid (R-2300TDI-R)SOD.
3. The stage of thermal imidization of the prepolymer to form coPUI (R-2300TDI-R)SOD.

Thermal imidization of the obtained prepolymers in N-methyl-2-pyrrolidone (NMP) solution was carried out in an inert atmosphere (argon) at 165°C for 3.5 h. Dean-Stark packing was

http://dx.doi.org/10.5772/intechopen.78625

used to remove the water that was emitted from the imidization (curing of the prepolymer) in the form of an azeotropic mixture with toluene. The temperature was then raised to 210°C to complete the imidization process.

To obtain nanocomposites, the polymer solutions prepared during the synthesis were used. In the first step, the prepared nanoparticle powder solutions in NMP—graphene, vapor-grown carbon nanofibers (VGCF), single-walled carbon nanotubes (SWCNTs), tungsten disulfide, and tungsten diselenide (WS_2 and WSe_2, correspondingly)—were dispersed in NMP by ultrasound. Then, synthesized polymer solution was added and mixed on a mechanical stirrer for 4 h. The nanoparticles are taken so that, after removal of the solvent, the amount of nanoparticles in the polymer is the required amount of percent by weight. Solutions of the resulting mixture were applied to a glass, polyimide (PI) film, fluoroplastic, and aluminum substrates. The resulting polymer coatings were dried at 80°C for 12 h and, then, heated stepwise at 120, 140, 160, and 180°C for 1 h at each step. The thickness of the heated films ranged from 100 to 300 μm.

It is known that imide-containing film coatings display strong adhesion to various substrates [26]. Some film samples were prepared on aluminum substrates. The coating samples formed on aluminum substrates were immersed in concentrated hydrochloric acid to remove the substrate, and then the resulting films were repeatedly washed in distilled water. The nanocomposite films based thereon containing from 1 to 10 wt.% carbon nanofillers of different morphologies—SWCNT, VGCF, graphene, and WS_2 and WSe_2 nanoparticles—were prepared.

2.2. Methods

The surface morphology of the synthesized copolymer films was investigated by the AFM method on the AFM device NT-206 (produced by "Microtestmashiny ODO," Belarus) using standard CSC38 and NSC11-type silicon probes with the radius of tip curvature less than 10 nm and stiffness of cantilever 0.08 and 3 N/m produced by "MikroMasch" (Estonia). The roughness, coefficient of friction, and friction force in nano- and microscale of samples were evaluated. The surface roughness was estimated in scanning areas of 2 × 2, 5 × 5, and 10 × 10 μm.

The friction force and friction coefficient (C_{fr}) were determined using 20 × 20 μm scanning areas with silicon probe NSC11 of V-shaped type with stiffness of cantilever 3 N/m at the moving speed 1.55 μm/s. The tip radius was specially blunted by pre-scanning to curvature 100 nm. Such preparation prevents the probe from further blunting and keeps the contact condition stable [8]. C_{fr} is calculated from a ratio of the force of friction between two bodies and the normal force pressing them together and their measurement as described previously [8, 10]. To measure the friction force, the AFM probe scans the surface in the so-called two-pass method [10]. During the first pass, the probe goes forward along the surface. When the probe returns back in the second pass, it moves according to the first line, which suits to the relief of the surface. During the forward and the back passes, the friction forces act from the surface on a tip, which cause the torsion of the cantilever besides the cantilever's deflection in the normal direction. The angle of this twist depends on the value of friction force. To calculate the effect of frictional forces more precisely, the angle of twist when the probe is moved in the forward and backward directions is divided in half [7, 8].

C_{fr} was determined in several regimes: on one scan field for one line in the forward and backward direction and so on the multiple scans (200–400) in one place. The measurements were carried out both at room temperature and at a temperature of 120°C. The heating was carried out directly during the scanning process using a thermoplatform placed on the AFM table. The thermoplatform is equipped with heaters and a feedback system with sensors, which allows controlling the heating and automatically reducing the voltage, if necessary, to maintain the set temperature.

To determine the local mechanical properties of prepared films based on multiblock coPUI, a 750 Ubi (Hysitron, USA) nanoindentator with a Berkovich indenter with a radius of curvature of R = 100 nm was used. Berkovich indenters are preferred than the Vickers geometry indenters because the latter is prone to undesired "roof" tip imperfections.

Since the physical-mechanical properties of polymers depend not only on the chemical composition and macromolecule structure but also on their orientation in the material and the distribution of the unordered amorphous and partially ordered crystalline phases, they cannot be characterized by a single value of the elasticity modulus (E) or microhardness (H) [11]. In this study, the local mechanical properties were analyzed as a dependence of the characteristic on the depth of penetration into material. For each sample, not less than 100 indentation curves were performed with an increasing load of 50–5000 μN in 50 μN increments, and the dependencies of the E and H on the depth of indentation were constructed from the results obtained.

In order to compensate the size effect of nanoindentation at shallow depths associated with the fact that at small penetration depths the Berkovich tip has the shape of a hemisphere rather than a pyramid, the nanoindentator was pre-calibrated according to a standard sample of fused quartz in a range of loads that were individually selected for each sample by the corresponding depths from 5 to 200 nm. This approach allows achieving a minimum standard deviation in the measurements of E and H.

3. Results and discussion

3.1. Carbon nanoadditive influence on the coPUI film morphology

Typical AFM 3D images of the coPUI matrices and nanocomposite surfaces are presented in **Figures 1** and **2**. It is clearly seen that both sides—free side and bottom side—of the synthesized films significantly differ in the surface morphology. It can be concluded that their morphology and, also, the structure are extremely sensitive to the substrate surface nature as well as to the formation process. Hence, the effect of additive (graphene and SWCNTs) influence on the film structure is also large, which is confirmed by AFM images (**Figures 1** and **2**). In our work, special attention was paid to the definition of roughness parameters: R_a, arithmetic mean; R_q, rms surface roughness.

According to the AFM image, free surface of coPUI (R-2300TDI-R)SOD film (**Figure 1a**) at scanning area of 1.5 × 1.5 μm is smooth (R_a = 1.0 nm, R_q = 1.3 nm) and exhibits grain morphology with a lot of pore nano- and meso-sizes. For scanning area of 2 × 2 μm, this film surface has a roughness R_a = 3.2 nm and R_q = 4.9 nm on the free surface and R_a = 3.1 nm and R_q = 4.0 nm on the surface adjacent to the substrate.

http://dx.doi.org/10.5772/intechopen.78625

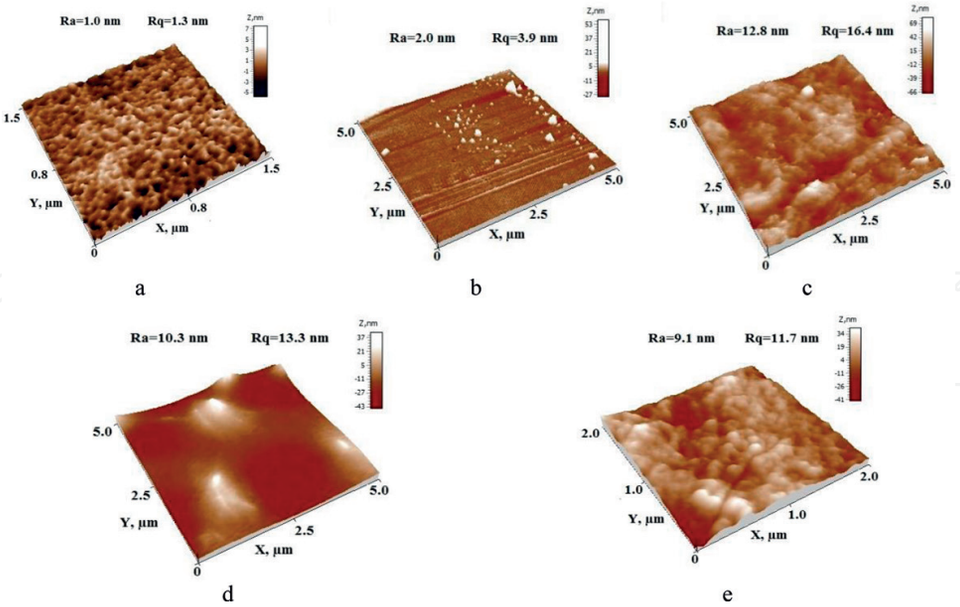

Figure 1. 3D images of (a) the coPUI(R-2300TDI-R)SOD matrix (side 1, scanning area 1.5 × 1.5 μm) and nanocomposites based thereon, (b) with 1 wt.% graphene (side 1, scanning area 5 × 5 μm), (c) with 1 wt.% graphene (side 2, scanning area 5 × 5 μm), (d) with 1 wt.% SWCNTs (side 1, scanning area 5 × 5 μm), and (e) with 1 wt.% SWCNTs (side 2, scanning area 2 × 2 μm). Glass substrate.

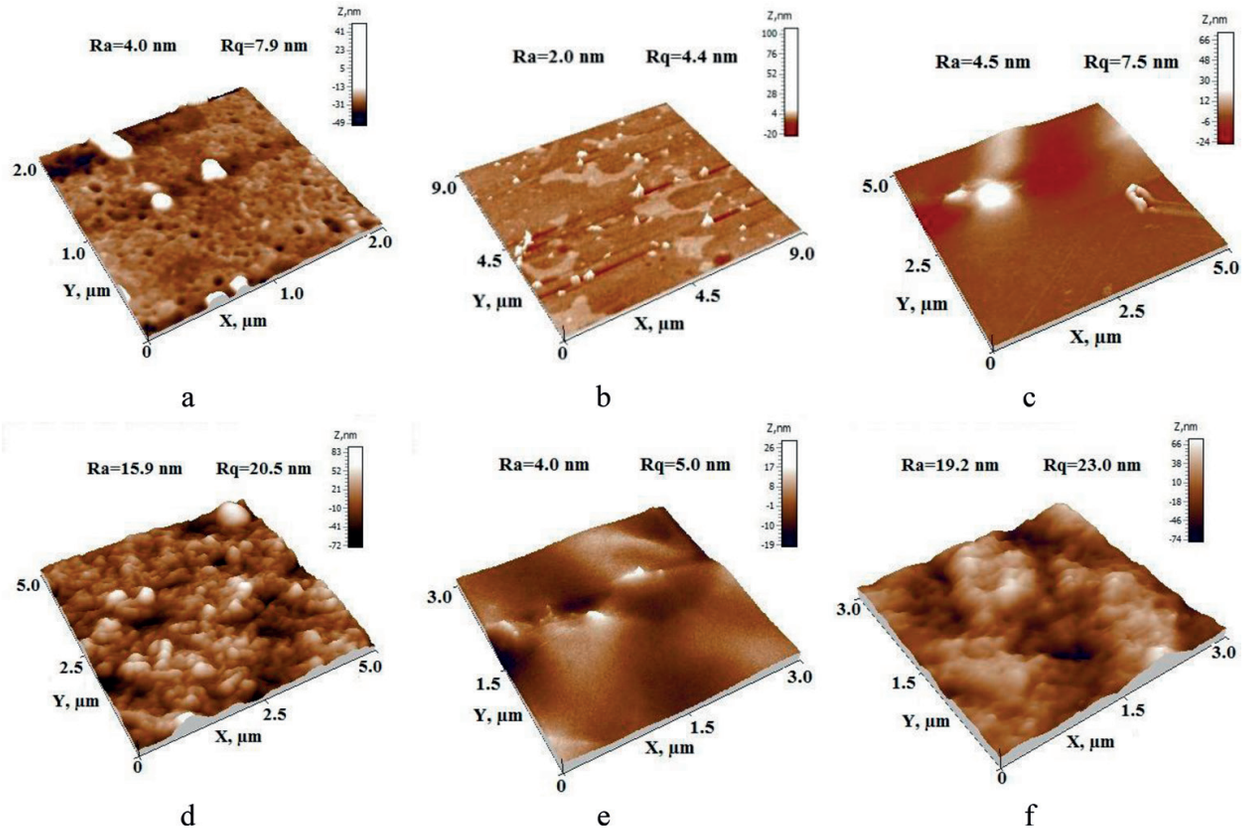

Figure 2. 3D images of the nanocomposites based on (R-AltTDI-R)SOD matrix: (a) matrix (side 1, scanning area 2 × 2 μm), (b) matrix with phase separation (side 1, scanning area 9 × 9 μm), (c) matrix with 1 wt.% VGCF (side 1, scanning area 5 × 5 μm), (d) matrix with 1 wt.% VGCF (side 2, scanning area 5 × 5 μm), (e) matrix with 1 wt.% SWCNTs (side 1, scanning area 3 × 3 μm), and (f) matrix with 1 wt.% SWCNT (side 2, scanning area 3 × 3 μm). Glass substrate.

For nanocomposites based on coPUI (R-2300TDI-R)SOD containing 1 wt.% graphene (**Figure 1b,c**), the great difference in morphology between free surface and surface adjacent to the substrate has been observed. The surface which was in contact with substrate (**Figure 1c**) looks more rough with roughness parameters R_a = 12.8 nm and R_q = 16.4 nm (for scanning area 5 × 5 μm) and R_a = 10.1 nm and R_q = 12.5 nm (for scanning area 2 × 2 μm). On the free surface of nanocomposite with 1 wt.% SWCNTs (**Figure 1d**), the ends of carbon nanotubes can be recognized. Again, the surface adjacent to the substrate is still rough and does not have homogeneous morphology like the free one (**Figure 1e**).

The significant difference in the topography of both coPUI nanocomposite film surfaces is clearly visible when comparing images in **Figure 1b–e**. Also, these surfaces exhibit a significant difference in the roughness values (**Table 1**).

Nanocomposite films of (R-2300TDI-R)SOD +1 wt.% graphene (**Figure 1b,c**) display the different roughness values between the film surfaces. When adding graphene, the free surface relief becomes coarser. It is likely that graphene nanoparticles are concentrated on one of the surfaces.

On the other hand, nanocomposite film of (R-2300TDI-R)SOD +1 wt.% SWCNT (**Figure 1d** and **e**) displays the close roughness values on both surfaces: R_a = 26.1 nm on the free surface and R_a = 26.5 nm on the surface adjacent to the substrate (for scanning area 5 × 5 μm). When the scanning area is reduced to 2 × 2 μm, the roughness values become several times smaller: R_a = 6.3 nm on the free surface and R_a = 11.9 nm on the surface adjacent to the substrate (**Table 1**). It can be concluded that the SWCNT is homogeneously distributed in composite volume.

For coPUI (R-2300TDI-R)SOD with 1 wt.% VGCF, the different roughness values between both surfaces were determined: R_a = 5.1 nm on the free surface and R_a = 23.1 nm on surface adjacent to the substrate (for scanning area 5 × 5 μm). When the scan area is reduced to 2 × 2 μm, the roughness values become R_a = 1.2 nm and R_q = 1.5 nm on the free surface and R_a = 13.8 nm and R_q = 18.0 nm on the surface adjacent to the substrate (**Table 1**).

Comparison of the roughness values for coPUI(R-2300TDI-R)SOD +1 wt.% VGCF films with all films of nanocomposites based on coPUI (R-AltTDI-R)SOD showed that they are about three times different (**Table 1**). Thus, additives significantly influence on the morphology formation of these coPUI films and on their surface properties.

The example of the phase separation on the free surface of coPUI (R-AltTDI-R)SOD film is clearly seen in **Figure 2b**. In the mode of lateral force contrast, light spots surrounded by dark polymer matrix have been observed that indicates a significant difference in the tribological properties of the phases in this sample.

3.2. Substrate nature influence on the coPUI film morphology

Substrate nature influence on the polymer film morphology can be traced comparing the surface morphology of coPUI (R-AltTDI-R) films prepared on three types of substrates: on a glass substrate, on the PI film substrate, and on a fluoroplastic substrate (**Figures 3–5**).

Figure 3 shows the AFM images of free surface (a–c) and surface adjacent to substrate (d–f) cast on a glass. A large number of pores with diameters from 50 to 200 nm are observed on both

http://dx.doi.org/10.5772/intechopen.78625

Polymer	Samples symbol	Film side	Scanning area (2 × 2 μm²)		Friction coefficients
			Roughness (R_a, nm)	Roughness (R_q, nm)	
(R-2300TDI-R)SOD {50}	50	1	3.2	4.9	0.164
		2	3.1	4.0	0.167
	50 + 1 wt.% VGCF	1	1.2	1.5	0.074
		2	13.8	18.0	0.061
	50 + 1 wt.% SWCNT	1	6.3	8.0	0.183
		2	11.9	14.9	0.185
	50 + 1 wt.% graphene	1	5.8	7.5	0.382
		2	10.1	12.5	0.170
	50 + 3 wt.% WS_2	1	13.5	16.9	0.262
		2	16.9	23.1	0.157
	50 + 1 wt.% WSe_2	1	9.3	14.2	0.158
		2	12.2	15.8	0.068
(R-AltTDI-R)SOD {45}	45	1	5.2	9.6	0.055
		2	6.2	7.9	0.065
	45 + 10 wt.% WS_2	1	3.4	4.9	0.179
		2	13.9	16.5	0.101
	45 + 10 wt.% WSe_2	1	16.5	21.9	0.107
		2	17.5	21.3	0.133
	45 + 1 wt.% VGCF	1	10.8	13.2	0.066
		2	14.1	18.1	0.071
	45+ 1 wt.% SWCNT	1	6.8	11.4	0.065
		2	25.4	31.1	0.063
	45 + 10 wt.% graphene	1	52.1	64.6	—
		2	14.4	18.2	0.092

Table 1. Comparison of the roughness and friction coefficient measurements using AFM in the contact mode for films and nanocomposites casted on a glass substrate.

surfaces, the pore depth at the free surface according to the profile (b) reaches ~2–8 nm, and at the surface to a glass substrate (e), it equals to 2–4 nm. The surface roughness differences are twofold (R_a = 0.9 nm and R_q = 1.1 nm for the surface adjacent to the substrate and R_a = 1.9 nm and R_q = 2.4 nm for the free surface). Therefore, both sides of the film look very similar.

Unlike a glass substrate, PI film substrate significantly changes surface topography (**Figure 4**). Thus, a lot of fine pores are not observed on the free surface. The surface adjacent to the substrate (d–f) is sufficiently smooth (R_a = 0.2 nm and R_q = 0.3 nm); a nanodomain morphology and a rather large number of nanopores with a depth not exceeding 1 nm are observed.

In **Figure 5**, AFM images of the film cast on the fluoroplastic substrate are given. The free surface (a–c) becomes more loose and nonuniform, and the roughness value (R_a = 5.8 nm and

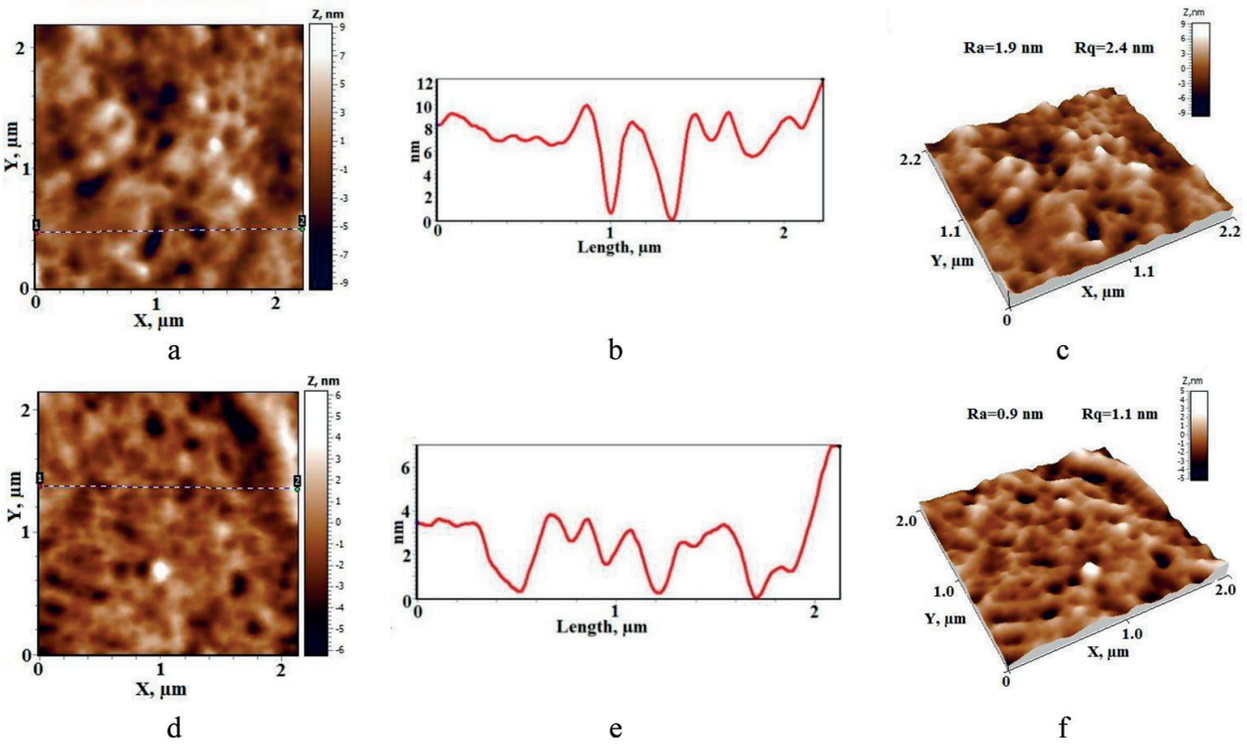

Figure 3. AFM images of coPUI (R-AltTDI-R)SOD film cast on a glass substrate: free surface (a–c) and surface adjacent to the substrate (d–f); (a,d) height images, (b,e) profile, and (c,f) 3D image.

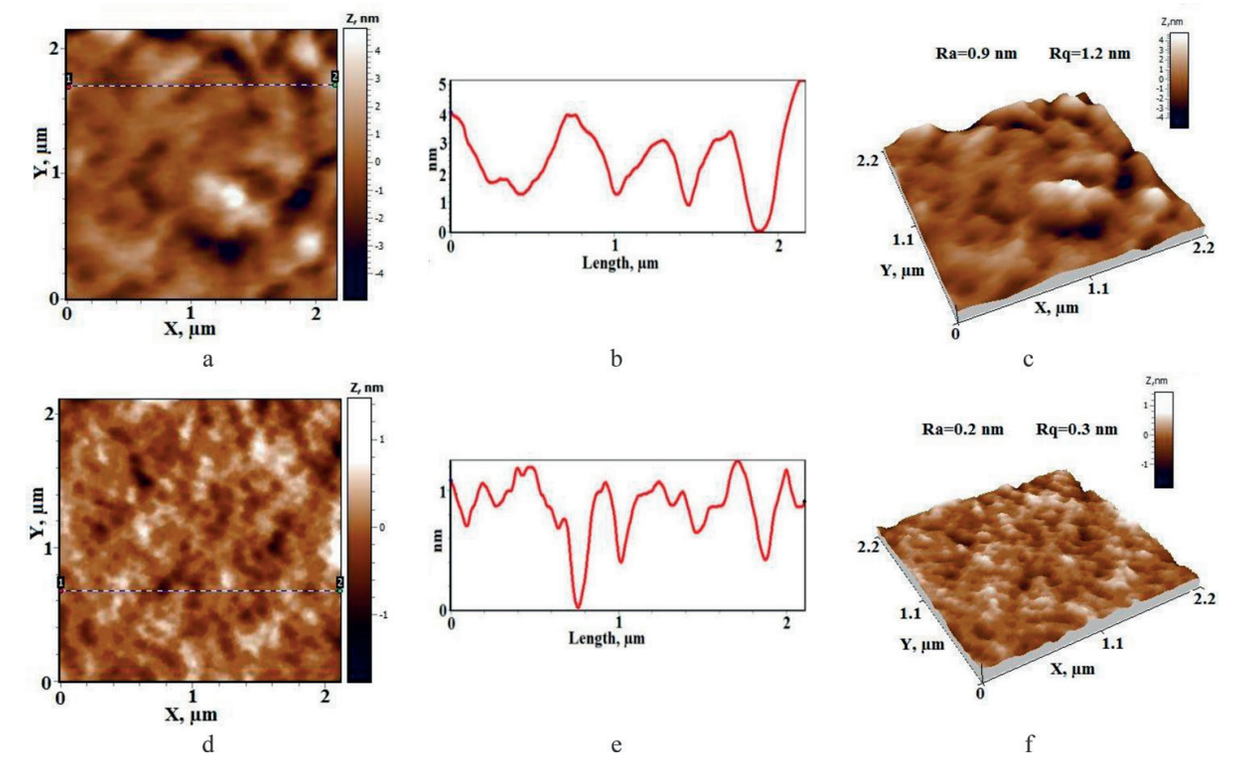

Figure 4. AFM images of coPUI (R-AltTDI-R)SOD film cast on a PI film substrate: free surface (a–c) and surface adjacent to the substrate (d–f); (a,d) height images, (b,e) profile, and (c,f) 3D image.

http://dx.doi.org/10.5772/intechopen.78625

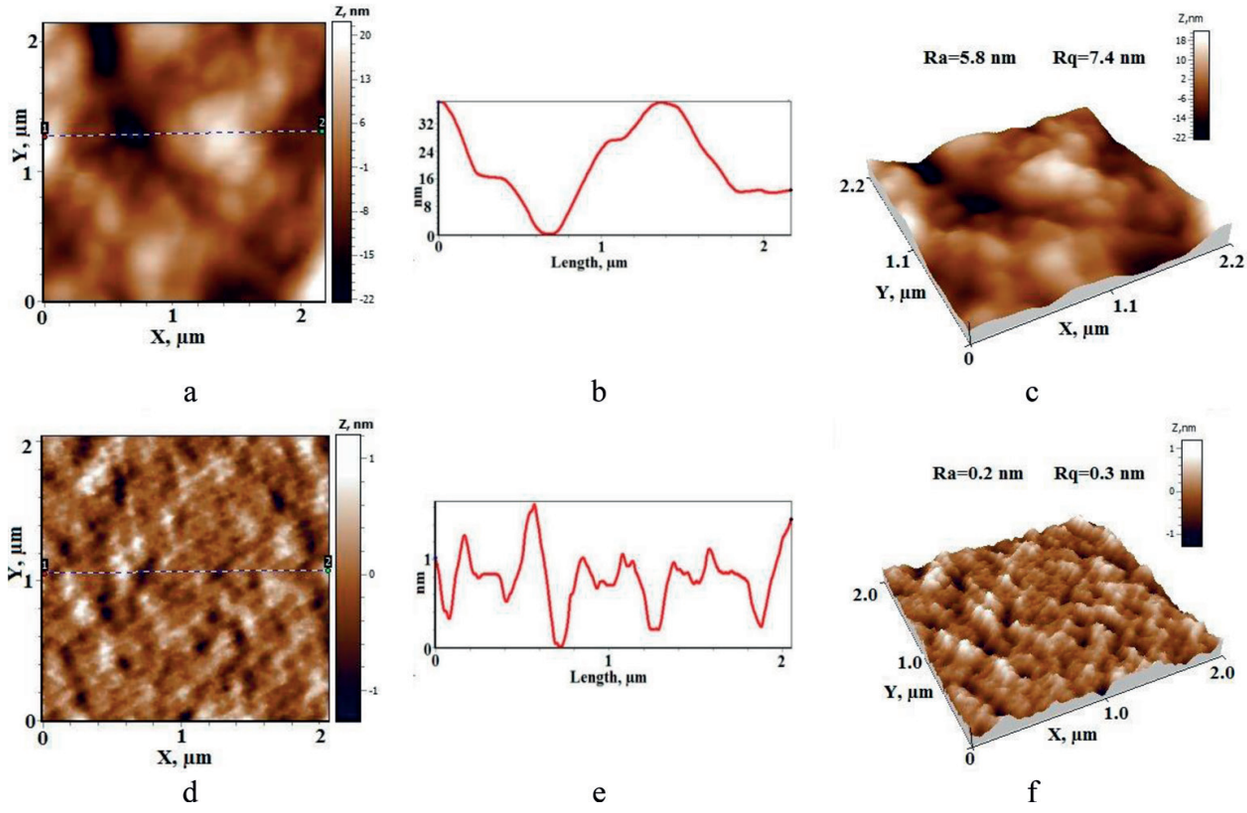

Figure 5. AFM images of coPUI (R-AltTDI-R)SOD film cast on a fluoroplastic substrate: free surface (a–c) and surface adjacent to the substrate (d–f); (a,d) height images, (b,e) profile, and (c,f) 3D image.

R_q = 7.4 nm) is significantly increased. As in the previous case, the surface adjacent to the substrate (d–f) has a nanodomain morphology and a large number of nanopores. Thus, it can be concluded that the nature of the substrate material on which the films are cast has a significant effect on the morphology of the sample.

3.3. Tribological characteristics of the coPUI films and nanocomposites

Friction coefficients (C_{fr}) of coPUIs based on (R-2300TDI-R)SOD and (R-AltTDI-R)SOD matrices modified by carbon nanomaterials determined by AFM method on one field are presented in **Figure 6**. C_{fr} of matrices without additives differ threefold: 0.164–0.167 for (R-2300TDI-R)SOD and 0.056–0.065 for (R-AltTDI-R)SOD.

The addition of VGCF reduces C_{fr} of (R-2300TDI-R)SOD matrix more than twice to 0.061–0.074 and leaves C_{fr} of (R-AltTDI-R)SOD matrix at the low level about 0.066–0.071. The addition of SWCNT practically leaves C_{fr} of both matrices on the level of C_{fr} of pure matrices.

On the other hand, the addition of graphene increases C_{fr} of both matrices especially of (R-2300TDI-R)SOD. Thus, only the addition of VGCF to (R-2300TDI-R)SOD matrix improves the tribological properties of the surface. The excess of the quantity necessary for the modification, as in the case of coPUI with 10 wt.% graphene, can substantially worsen the surface properties.

Friction coefficients of coPUIs based on (R-2300TDI-R)SOD and (R-AltTDI-R)SOD matrices modified by WS_2 and WSe_2 nanoparticles determined by AFM method on one field are

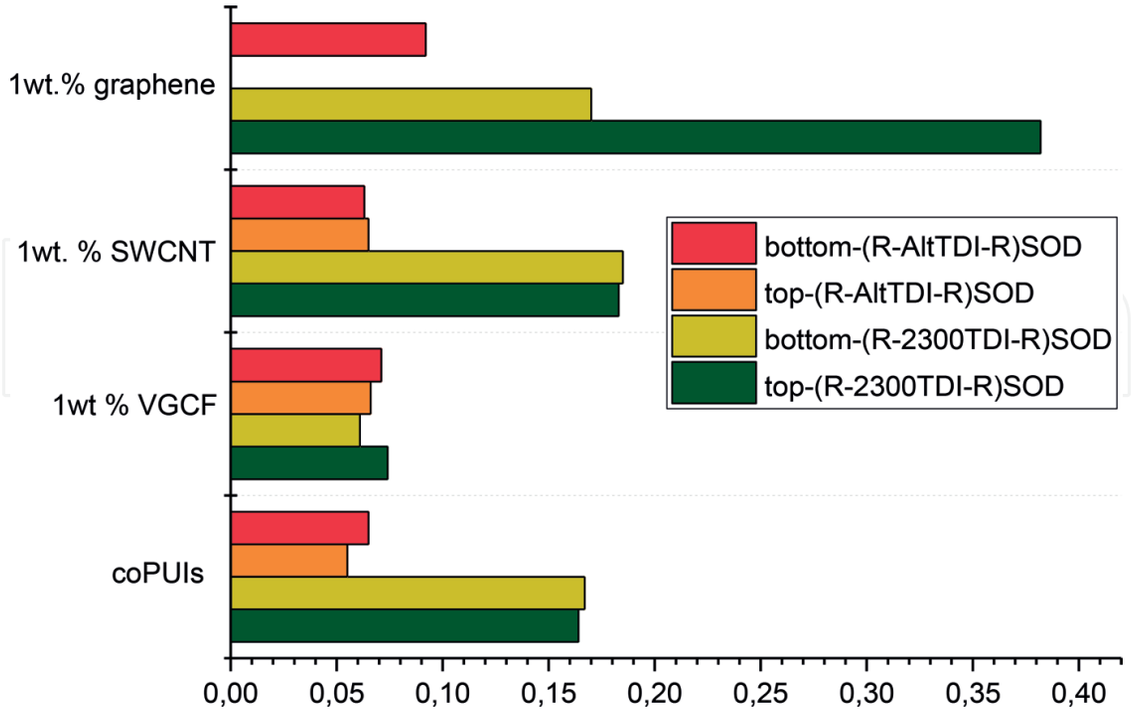

Figure 6. Friction coefficients of coPUIs based on (R-2300TDI-R)SOD (50) and (R-AltTDI-R)SOD (45) matrices and composites with carbon nanofillers as determined by AFM method in the contact mode on one field: matrices 50 and 45 without additives, matrices with 1 wt.% VGCF, matrices with 1 wt.% SWCNTs, and matrices with 1 wt.% graphene.

presented on **Figure 7**. In general, WS_2 and WSe_2 nanoparticles degrade C_{fr} of the (R-2300TDI-R) SOD and (R-AltTDI-R)SOD matrices due to a significant increase in roughness. WSe_2 decreases twice the C_{fr} of (R-AltTDI-R)SOD matrix surface casted on a glass substrate.

The results of C_{fr} changing during multi-pass tribological AFM testing of coPUI (R-AltTDI-R) SOD matrix as a dependence of "C_{fr}—number of scans" are presented in **Figure 8** (black solid line). This measurement was performed at 20°C and normal load about 175 nN. Friction forces were determined in a range of 10–160 nN. Each point on the C_{fr} graph (black solid line) and the roughness graph (blue solid line) was obtained from a separate AFM sequential scanning field (**Figure 8**).

At the initial stage of C_{fr} graph up to 50 cycles, the growth of C_{fr} to a value 0.9 was determined (black solid line), and the roughness values simultaneously decreased (blue solid line). When the probe moves along the surface, the roughness is smoothed out (blue solid line). The low initial value of C_{fr} 0.1 can be explained by the fact of developed roughness. In this cause the contact of the probe with the surface occurs along the tops of the irregularities. In this case, the contact area of the probe and the surface are composed of a plurality of point contacts, and the frictional forces are lower than in case when the smoothed sample contacts with entire surface of the probe. The energy should be spent on the process of smoothing, and it needs to apply a greater lateral force for further movement. Therefore, C_{fr} grows on this side. In the process of friction, the irregularities are smoothed out, and after reaching a minimum of roughness, the C_{fr} decreases over the next 100 cycles to a stable value of 0.05 (black solid line). And then, the mechanism of elastic non-wear friction works.

http://dx.doi.org/10.5772/intechopen.78625

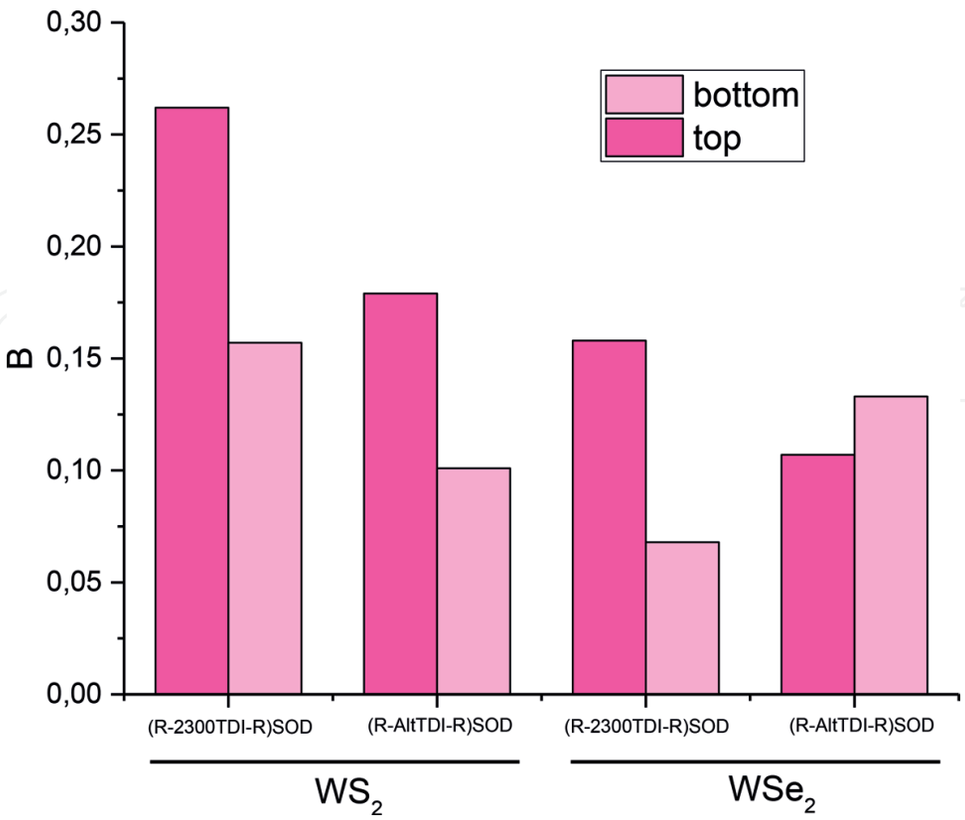

Figure 7. Friction coefficients of coPUIs based on (R-2300TDI-R)SOD (50) and (R-AltTDI-R)SOD (45) matrices modified by WS_2 and WSe_2 nanoparticles, determined by AFM method in the contact mode on one field.

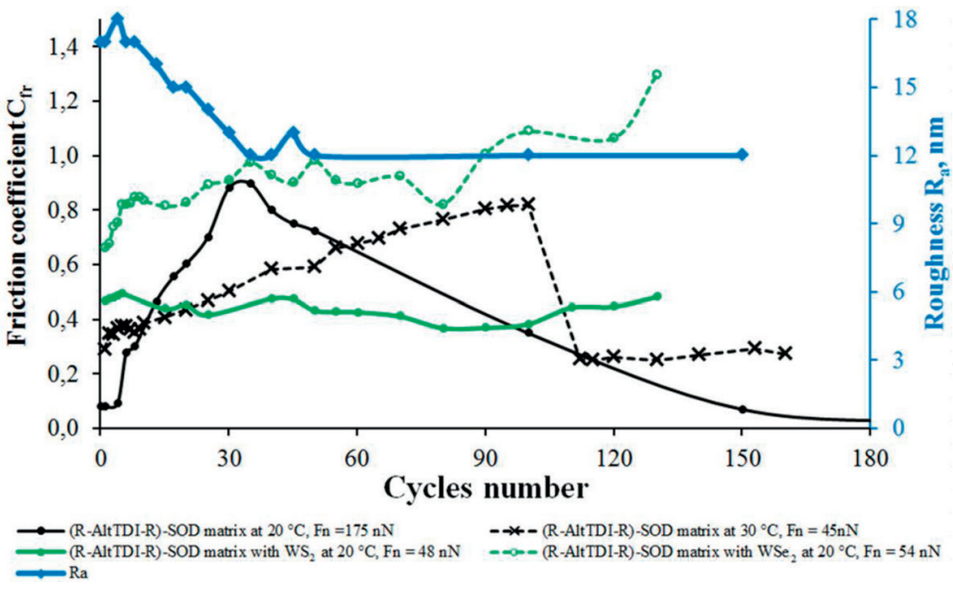

Figure 8. The results of coefficient of friction (C_{fr}) and roughness (R_a) changing during multi-pass tribological AFM testing of (R-AltTDI-R)SOD matrix: C_{fr} of pure matrix at 20°C and F normal = 175 nN (black solid line), C_{fr} of pure matrix at 30°C and F normal = 45 nN (black-dashed line), C_{fr} of matrix with WS_2 at 20°C and F normal = 48 nN (green solid line), C_{fr} of matrix with WSe_2 at 20°C and F normal = 54 nN (green-dashed line), and roughness (R_a) of pure matrix at 20°C and F normal = 175 nN (blue solid line).

When the same multi-pass tests are repeated at the room temperature about 30°C, the probe-sample contact conditions change, which raises the initial value of C_{fr} to 0.3 instead of 0.1 at 20°C (**Figure 8**, black-dashed line). Then, normal load was about 116 nN, and friction forces were determined in range 30–92 nN. The further stages of the curve also change somewhat. C_{fr} is stable at the beginning during the first 10 cycles, and then it increases smoothly to 0.8 (black solid line). After reaching this value at 110 cycles as well as at 20°C, the curve decreases to a stable level about 0.25 (black solid line). The testing at 30°C places peculiarities on the C_{fr} graph: the growth of values is smoother, and the decrease is faster.

The results of coefficient of friction changing during multi-pass tribological AFM testing at 30°C of (R-AltTDI-R)SOD matrix with WS_2 and WSe_2 nanoparticles are shown in **Figure 8** (green lines). As for the pure (R-AltTDI-R)SOD matrix, the results of testing at higher temperature show the increased value of C_{fr} in comparison with the testing at 30°C (**Figure 8**, black-dashed line). The addition of WS_2 keeps the value C_{fr} stable on the level 0.45 (green solid line). The addition of WSe_2 leads to the increase of C_{fr} (green-dashed line).

Comparing the similar values of C_{fr} for (R-AltTDI-R)SOD matrix determined in regimes "multi-pass scan" and "one scan under heating," it should be noticed that the influence of heating in a range of 75–85°C on the surface properties is similar to the influence of 200–400 scans of multi-pass testing at 20°C [8]. This fact allows to make a conclusion that there is heating in this micro-contact equal to 75°C.

These results show that synthesized modified coPUI films are very promising for tribological applications, and their properties can be controlled both by temperature and by mechanical action.

The influence of heating on C_{fr} for (R-AltTDI-R)SOD with WSe_2 addition has been shown in our previous work [8]. It was found that C_{fr} keeps stable at the level of 0.30–0.35 till 45°C. Then, it dramatically decreases up to 0.05 at 60°C and keeps stable till 70°C. Again, at 75°C it decreases till 0.01.

3.4. Nanoindentation of coPUI films

On the dependence of E on the depth of indentation for coPUI (R-2300TDI-R)SOD, two curves are characteristic for the material. It can be concluded that there is a less elastic phase on the surface layer and a more elastic phase in the depth—in bulk material (**Figure 9**, blue curves). In this case, the microhardness for coPUI (R-2300TDI-R)SOD has a unimodal distribution in values from 2 to 4 MPa, and one curve (**Figure 9**, red curves) is present on the plots of the microhardness versus the depth of indentation. Different markers denote the values obtained from different sides of the films. For microhardness they are very close, and for the elastic modulus completely coincide.

On the other hand, coPUI (R-AltTDI-R)SOD is characterized by unimodal distributions for both E and H (**Figure 10**). The transition from the surface to the depth of the sample decreases both for E from 6 to 3 GPa and for H from 400 to 200 MPa.

The performed studies of the samples of synthesized coPUI showed that the values of H and E measured on both sides of the films are practically the same, and when the dependencies obtained from different sides of the films coincide in one plot, for each coPUI they almost

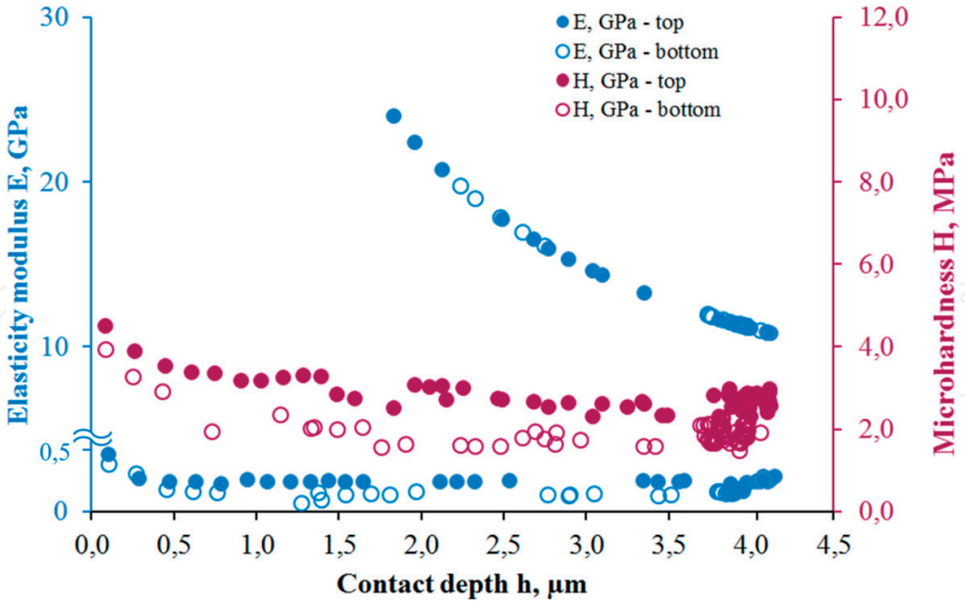

Figure 9. Dependencies of elasticity modulus (blue curves) and microhardness (red curves) versus the depth of indentation for the coPUI (R-2300TDI-R)SOD without nanofillers.

completely coincide, forming exponential curves. The values of E and H for film cast on glass and fluoroplastic substrates are identical, despite the different microstructure of the surface, so hereinafter we consider the values obtained for films prepared on a glass substrate.

With the addition of 1 wt. % SWCNTs, the initial values of E and H for coPUI (R-2300TDI-R) SOD practically do not change (**Figure 11**). For the "amorphous" phase on top of the film E is 25 MPa and from below 20 MPa. At the same time, H is on the top of 3 MPa and from the bottom 2 MPa. For the "partially ordered" phase, E varies from 11 to 14 GPa from the top, from 10 to 22 GPa from the bottom, and from the top and H from below from 1.5 to

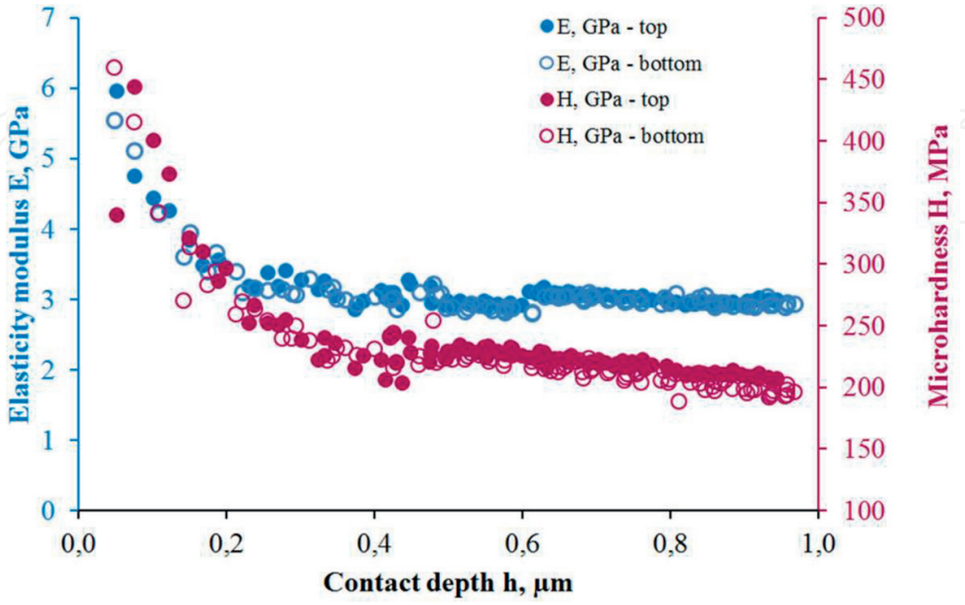

Figure 10. Dependencies of elasticity modulus (blue curves) and microhardness (red curves) versus the depth of indentation for the coPUI (R-AltTDI-R)SOD without nanofillers.

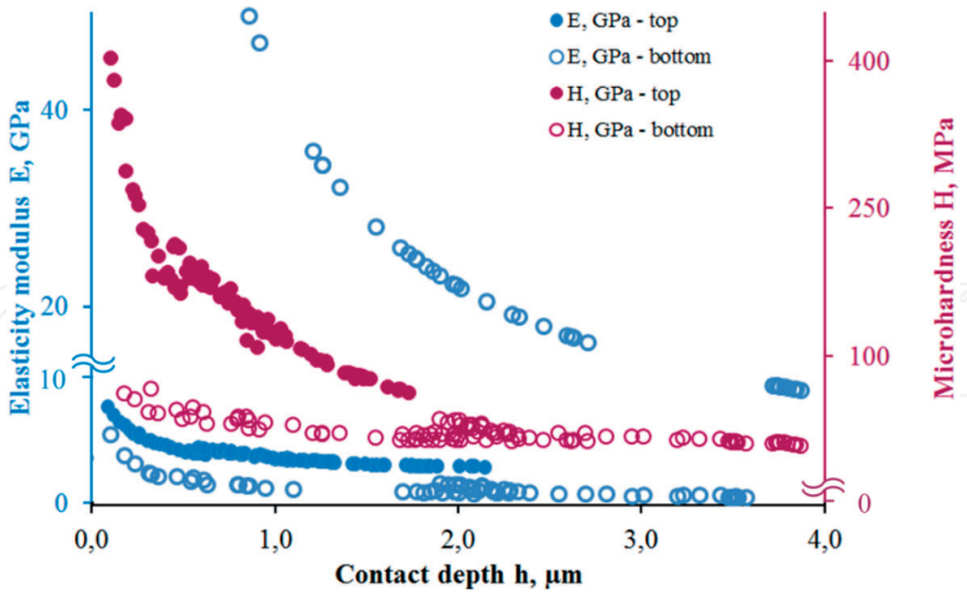

Figure 11. Dependencies of elasticity modulus (blue curves) and microhardness (red curves) versus the depth of indentation for the coPUI (R-2300TDI-R)SOD with 1 wt.% SWCNTs.

2.5 MPa. The microstructure of the surface remains unstructured, which is characteristic for polymers in the amorphous state.

The amorphous phase on the upper surface of the film practically does not change. The depth of the "partially ordered" phase changes: it moves closer to the free surface (**Figure 11**). From below, the depth of the location of the "partially ordered" phase remained unchanged. For an amorphous phase from below, the values of E and H increased by a factor of 2: E was 20 MPa and became 40 MPa, and H was 2 MPa and became 4 MPa.

The greatest changes in the properties of coPUI (R-2300TDI-R)SOD were detected with the addition of 1 wt.% SWCNTs. The "partially ordered" phase (or moved to a depth greater than 4 μm) completely disappeared from the top, and from the bottom, it was preserved and moved closer to the surface than in the coPUI without SWCNTs (**Figure 12a**). The E is 10–20 GPa. For an amorphous phase, the E film increased 10 times from the top—it was 35 MPa and became 350 MPa. The H of the amorphous phase increased 23-fold: from 3 to 70 MPa. From the bottom of the film, the values of H and E increased by 5 and 10 times: E was 20 MPa and became 100 MPa, and H was 2 MPa and became 20 MPa. The microstructure of the surface is structured, with noticeable linear formations in perpendicular directions in the plane (**Figure 12d** and **e**).

The introduction of all types of nanofillers in an amount of 1 wt.% practically did not change the mechanical properties of the coPUI (R-AltTDI-R)SOD. In our experiments only the addition of graphene in an amount about 10 wt.% lowered the properties of this for coPUI (R-AltTDI-R)SOD by a factor of 1.5. In general, the material with 10 wt.% graphene is unstable due to the accumulation of excess graphene in the form of submicron-sized inclusions. The surface microstructure of the composite became nanostructured.

As a result, it was established that the coPUI (R-2300TDI-R)SOD and coPUI (R-AltTDI-R)SOD are radically different in the distribution of the elasticity modulus E: coPUI (R-2300TDI-R)SOD has a bimodal distribution (**Figure 13a**), and for coPUI (R-AltTDI-R)SOD, it is unimodal (**Figure 13b**).

http://dx.doi.org/10.5772/intechopen.78625

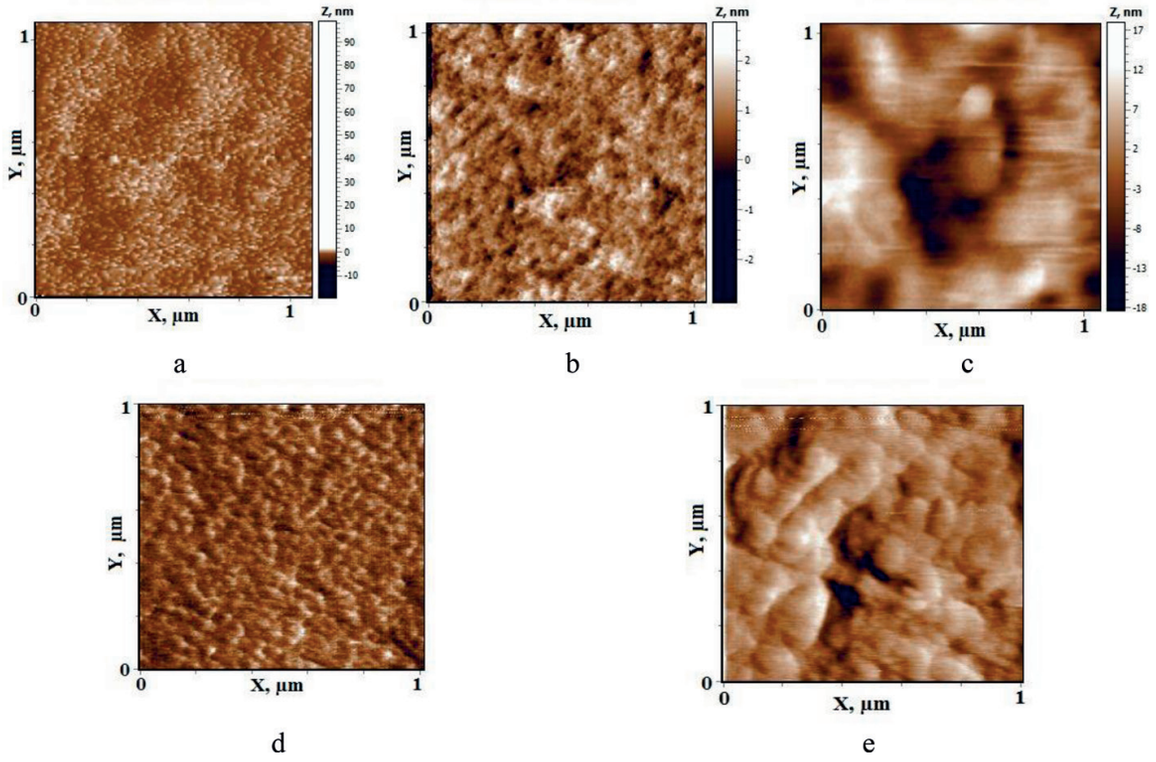

Figure 12. AFM images of the surface microstructure of the coPUI (R-2300TDI-R)SOD: (a) the initial matrix (free side), (b) matrix with 1 wt.% graphene (free side), (c) the side from the substrate, (d) matrix with 1 wt.% SWCNTs (free side), and (e) side from the substrate; scan area 1 × 1 µm.

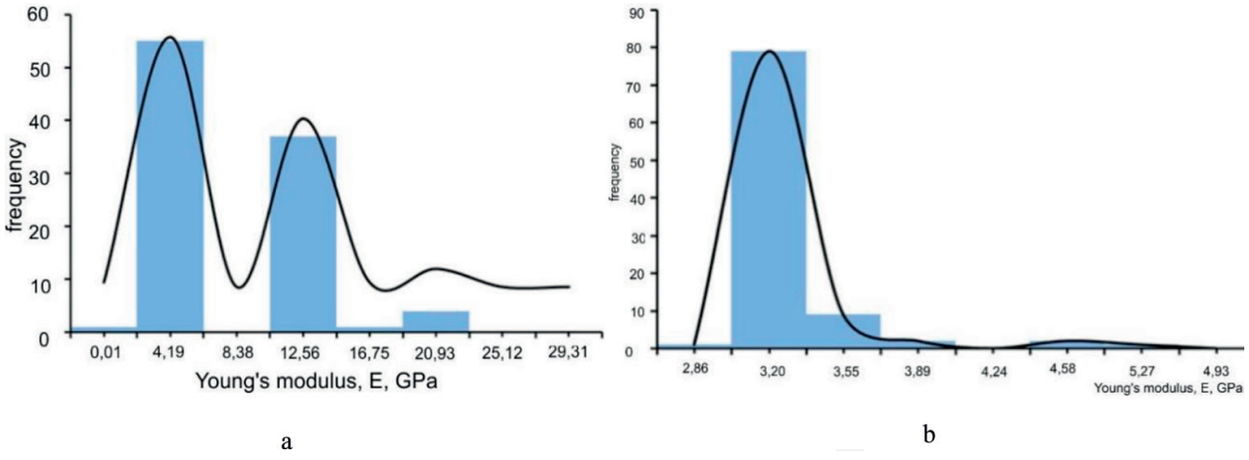

Figure 13. Types of elastic modulus distribution: (a) bimodal for coPUI (R-2300TDI-R)SOD and (b) unimodal for coPUI (R-AltTDI-R)SOD.

So, the dependencies of the modulus of elasticity and microhardness on the insertion depth for synthesized coPUI (R-2300TDI-R)SOD and (R-AltTDI-R)SOD showed that the investigated coPUI differs dramatically in terms of the values of the physical-mechanical characteristics and the type of their distribution. The wide range of values of E is typical for coPUI (R-2300TDI-R)SOD nanocomposites—up to 35 GPa within the surface layers—that may be explained by the presence of a partially ordered phase near the surface, which is extremely sensitive both to the synthesis conditions (the evaporation rate of the solvent) and to surface

effects. Contrary, coPUI (R-AltTDI-R)SOD is characterized by greater uniformity of values (up to 4 GPa) and higher microhardness (up to 0.45 GPa). Again, this sensitivity makes it possible to vary the localization of the phase by introduction of carbon nanofillers. The greatest changes in the elastic properties of coPUI (R-2300TDI-R)SOD nanocomposites were detected with the addition of 1 wt.% SWCNTs.

4. Conclusions

The morphology, tribological, and local mechanical properties of new copolyurethane-imides (coPUIs) and nanocomposites based thereof were studied by AFM and NI methods. AFM method in the contact mode of lateral forces revealed the presence of different phases on the surface of synthesized samples. A relationship has been established between the presence of various contrast phases and the chemical structure of the monomers used for synthesis. The ability to control the roughness at the nanoscale for coPUI films on a free surface and on the surface adjacent to substrate is established, using solid substrates of various natures. These characteristics are very important for obtaining materials with improved tribological properties. The AFM and NI methods have shown that the adhesion force and the specific surface energy for synthesized coPUIs increase exponentially with an increase in the normal loading during indentation.

The NI method established the phase separation of coPUI films, which leads to significantly different values of the microhardness on both sides of the copolymer films. The microhardness on the free surface (facing to the air) is much higher than the microhardness of the surface adjacent to the solid support. These results indicate the importance of controlling the microhardness of both film surfaces at nano- and microscales.

Dependencies of microhardness and modulus of elasticity on the depth of indentation have been obtained for initial coPUI (P-2300TDI-P)SOD and coPUI (R-AltTDI-R)SOD and nanocomposites based thereof containing SWCNTs, graphene, and carbon nanofibers. It was found in our case that for each synthesized coPUI, there is only one type of carbon nanomaterials that exerts the greatest influence on their characteristics. Thus, for coPUI (R-AltTDI-R)SOD, it is graphene, the introduction of which leads to an increase in the modulus of elasticity on the free surface up to 4.14 GPa, and for coPUI (R-2300TDI-R)SOD, it is SWCNT, but in this case, the maximum values of the elastic modulus E = 42.82 GPa are observed on the surface adjacent to the substrate.

Analysis of the tribological characteristics of nanocomposites based on coPUI (P-2300TDI-P) SOD showed that VGCF exerts the greatest effect on the decrease in C_{fr} and their introduction in amounts about 1 wt.% leads to a decrease in C_{fr} practically by a factor of 2. On the other hand, when VGCF is introduced into the coPUI (R-AltTDI-R)SOD, C_{fr} remains practically unchanged. And, when this coPUI is filled with graphene, an increase in C_{fr} is observed, apparently because of a significant increase in the roughness of the surface of nanocomposite films.

Since the initial coPUI (P-2300TDI-P)SOD and coPUI (R-AltTDI-R)SOD films exhibit radically different values of the friction coefficient, C_{fr} = 0.362 and 0.174 for coPUI (P-2300TDI-P) SOD and C_{fr} = 0.055 and 0.066 for coPUI (R-AltTDI-R)SOD, the introduction of WS_2 or WSe_2 nanoparticles leads to different effects. Nanocomposites based on coPUI (R-2300TDI-R)SOD with both types of nanoparticles have lower C_{fr} values than the copolymer matrix, while WSe_2 nanoparticles have a greater effect on tribological properties of this coPUI and reduce the C_{fr}

more than twice. Conversely, the initial coPUI (R-AltTDI-R)SOD has a sufficiently low C_{fr}, and the introduction of nanoparticles WS_2 and WSe_2 leads to its almost doubling.

The efficiency of multi-pass scanning tests is shown for investigating the tribological properties of modified copolymer systems. It is found that coPUI (R-AltTDI-R)SOD and nanocomposites based thereof with SWCNT have the best tribological properties, while SWCNTs are uniformly distributed in the material and cause homogeneous structuring at the nanolevel. As a result of studying the tribological properties of coPUI film surface using AFM method with multi-pass scanning, it has been found that effective methods for improving these properties can be either modification by SWCNTs (up to 1 wt.%) or heating to 30°C.

Our results show that synthesized coPUI films and nanocomposites based thereof are very promising materials for tribological applications and their physical-mechanical properties can be controlled both by temperature and by mechanical action.

Acknowledgements

This research was supported by the grants of the Russian Foundation for Basic Research (RFBR) No. 16-53-00178 and the Belarusian Republican Foundation for Fundamental Research (BRFFR) No. F16R-142.

Author details

Tatiana Evgenievna Sukhanova[1,3]*, Tatyana A. Kuznetsova[2], Vasilina A. Lapitskaya[2], Tatiana I. Zubar[2], Sergei A. Chizhik[2], Milana E. Vylegzhanina[3], Aleksandr A. Kutin[3], Andrey L. Didenko[3] and Valentin M. Svetlichnyi[3]

*Address all correspondence to: tat_sukhanova@mail.ru

1 Federal State Unitary Enterprise "S.V. Lebedev Institute of Synthetic Rubber", Saint-Petersburg, Russia

2 A.V. Luikov Heat and Mass Transfer Institute NAS Belarus, Minsk, Belarus

3 Institute of Macromolecular Compounds of the Russian Academy of Sciences, Saint-Petersburg, Russia

References

[1] Al-Ajaj I, Kareem A. Synthesis and characterization of polyimide thin films obtained by thermal evaporation and solid state reaction. Materials Science—Poland. 2016; **34**:132-136

[2] Anishchik V, Uglov V, Kuleshov A, Filipp A, Rusalsky D, Astashynskaya M, Samtsov M, Kuznetsova T, Thiery F, Pauleau Y. Electron field emission and surface morphology of a-C and a-C:H thin films. Thin Solid Films. 2005;**482**:248-252

[3] Zavaleyev V, Walkowicz J, Kuznetsova T, Zubar T. The dependence of the structure and mechanical properties of thin ta-C coatings deposited using electromagnetic venetian blind plasma filter on their thickness. Thin Solid Films. 2017;**638**:153-158

[4] Kuznetsova TA, Chizhik SA, Khudoley AL. Deformation structuring of aluminum films upon microindentation. Journal of Surface Investigation. 2014;**8**(6):1275-1285

[5] Kuznetsova TA, Zubar TI, Sudilovskaya KA, Chizhik SA, Didenko AL, Svetlichnyi VM, Sukhanova TE, Vylegzhanina ME. Investigation of the surface of polymer thermoplastic elastomers with detection of various phases in the lateral forces regime. In: XII Intern. Conf Methodological Aspects of Scanning Probe Microscopy; Minsk: Belaruskaya Navuka; 2016. pp. 137-143

[6] Sukhanova TE, Kuznetsova TA, Vylegzhanina ME, Svetlichnyi VM, Zubar TI, Chizhik SA. Possibilities of using probe methods in the diagnostics of nanomodified thermoplastic elastomers. In: XII Intern. Conf. Methodological Aspects of Scanning Probe Microscopy; Minsk: Belaruskaya Navuka; 2016. pp. 8-17

[7] Chizhik SA, Rymuza Z, Chikunov VV, Jarzabek D, Kuznetsova T. Micro- and nanoscale testing of tribomechanical properties of surfaces. In: Jabłoński R, et al., editors. Recent Advances in Mechatronics. Berlin, Heidelberg: Springer; 2007. pp. 541-545

[8] Kuznetsova TA, Zubar TI, Lapitskaya VA, Sudzilouskaya KA, Chizhik SA, Didenko AL, Svetlichnyi VM, Vylegzhanina ME, Kudryavtsev VV, Sukhanova TE. Tribological properties investigation of the thermoplastic elastomers surface with the AFM lateral forces mode. IOP Conference Series: Materials Science and Engineering. 2017;**256**(012022):114-119

[9] Vylegzhanina ME, Kuznetsova TA, Didenko AL, Zubar T, Sudilovskaya KA, Svetlichnyi VM, Kudryavtsev VV, Chizhik SA, Sukhanova TE. Investigation of nanomaterials based on imide-containing thermoplastic elastomers using AFM methods and nanoindentation. In: XXIV Rus. Conf. On Electron Microscopy (RCEM-2016); 2016. pp. 250-251

[10] Bhushan B, Israelachvili JN, Landman U. Nanotribology: Friction, wear and lubrication at the atomic scale. Nature. 1994;**374**:607-616

[11] Diez-Pascual AM, Gomez-Fatou MA, Ania F, Flores A. Nanoindentation in polymer nanocomposites. Progress in Materials Science. 2015;**67**:1-94

[12] Gerkin RM, Hilker BL. Block copolymers: Segmented. In: Buschow KHJ, et al. editors. Encyclopedia of Materials: Science and Technology. 2nd ed. Amsterdam, New York: Elsevier; 2001. pp. 730-732

[13] Yilgör I, Yilgör E, Wilkes GL. Critical parameters in designing segmented polyurethanes and their effect on morphology and properties: A comprehensive review. Polymer. 2015; **58**:A1-A36

[14] Banu P, Radhakrishnan G. Unsaturated poly(ester-imide)s from hydroxyl-terminated polybutadiene, dianhydride and diisocyanate. European Polymer Journal. 2004;**40**: 1887-1894

[15] Banu P, Radhakrishnan G. Thermoplastic poly(esterimide)s derived from anhydride terminated polyester prepolymer and diisocyanate. Journal of Polymer Science, Part A: Polymer Chemistry. 2004;**42**:341-350

[16] Philip Gnanarajan T, Sultan Nsser A, Padmanabha Iyer N, Radhakrishnan G. Synthesis of poly(urethane-imide) using aromatic secondary amine-blocked polyurethane prepolymer. Journal of Polymer Science, Part A: Polymer Chemistry. 2000;**38**:4032-4037

[17] Krijgsman J, Husken D, Gaymans R. Synthesis and properties of thermoplastic elastomers based on PTMO and tetra-amide. Polymer. 2003:7573-7588

[18] Sukhanova TE, Vylegzhanina ME, Didenko AL, Svetlichnyi VM, Gofman IV, Volkov AY, Kutin AA, Yakushev PN, Bershtein VA. Influence of the introduction of carbon nanoparticles on the structure, morphology and properties of nanocomposites based on copolyurethane-imides. In: XXI Intern. Symp. "Nanophysics and Nanoelectronics", Vol. 1; 2017. pp. 331-332

[19] Sukhanova TE, Vylegzhanina ME, Kuznetsova TA, Svetlichnyi VM, Didenko AL, Shiryaeva TI, Kutin AA, Volkov AYa, Kudryavtsev VV, Chizhik SA. Complex diagnostics of morphology and local mechanical characteristics of hybrid materials based on multiblock (segmented) PEI and MQ-resins by AFM methods and nanoindentation. In: 16th Intern. Symp. "Nanophysics and Nanoelectronics", V. 1; 2015. pp. 292-296

[20] Vylegzhanina ME, Kuznetsova TA, Didenko AL, Zubar T, Sudilovskaya KA, Svetlichnyi VM, Kudryavtsev VV, Chizhik SA, Sukhanova TE. Investigation of nanomaterials based on imide-containing thermoplastic elastomers using AFM methods and nanoindentation. In: XXIV Rus. Conf. On Electron Microscopy (RCEM-2016); 2016. pp. 250-251

[21] US Patent 4929358. Polyurethane-imide membranes and their use for the separation of aromatics from non-aromatics; 1990

[22] US Patent 4944880. Polyimide/Aliphatic Polyesters Copolymers; 1994

[23] Didenko A, Yudin V, Smirnova V, Gofman I, Popova E, Elokhovskii V, Svetlichnyi V, Kudryavtsev V. Modification of the thermoplastic polyheteroarylenes with aliphatic polyethers and polyesters: synthesis and dynamic mechanical properties. Materials, Methods & Technologies. 2014;**8**:31-40

[24] Yudin VE, Bugrov AN, Didenko AL, Smirnova VE, Gofman IV, Kononova SV, Kremnev RV, Popova EN, Svetlichnyi VM, Kudryavtsev VV. Composites of multiblock (segmented) aliphatic poly(ester imide) with zirconia nanoparticles: Synthesis, mechanical properties, and pervaporation behavior. Polymer Science Series B. 2015;**56**(6):919-926

[25] Yudin VE, Smirnova VE, Didenko AL, Popova EN, Gofman IV, Zarbuev AV, Svetlichnyi VM, Kudryavtsev VV. Dynamic mechanical analysis of multiblock (segmental) polyesterimides. Russian Journal of Applied Chemistry. 2013;**86**(6):920-927

[26] Bessonov MI, Koton MM, Kudryavtsev VV, Laius LA. Polyimides Thermally Stable Polymers. N.Y: Consultants Bureau; 1987. 318 p

IntechOpen